
NEURALFMU: PRESENTING A WORKFLOW FOR INTEGRATING HYBRID NEURALODES INTO REAL WORLD APPLICATIONS

PREPRINT

Tobias Thummerer
Chair of Mechatronics
Augsburg University
tobias.thummerer@uni-a.de

Johannes Stoljar
Chair of Mechatronics
Augsburg University
johannes.stoljar@uni-a.de

Lars Mikelsons
Chair of Mechatronics
Augsburg University
lars.mikelsons@uni-a.de

ABSTRACT

The term *NeuralODE* describes the structural combination of an Artificial Neural Network (ANN) and a numerical solver for Ordinary Differential Equations (ODEs), the former acts as the right-hand side of the ODE to be solved. This concept was further extended by a black-box model in the form of a Functional Mock-up Unit (FMU) to obtain a subclass of NeuralODEs, named *NeuralFMUs*. The resulting structure features the advantages of first-principle and data-driven modeling approaches in one single simulation model: A higher prediction accuracy compared to conventional First Principle Models (FPMs), while also a lower training effort compared to purely data-driven models. We present an intuitive workflow to setup and use NeuralFMUs, enabling the encapsulation and reuse of existing conventional models exported from common modeling tools. Moreover, we exemplify this concept by deploying a NeuralFMU for a consumption simulation based on a Vehicle Longitudinal Dynamics Model (VLDM), which is a typical use case in automotive industry. Related challenges that are often neglected in scientific use cases, like real measurements (e.g. noise), an unknown system state or high-frequent discontinuities, are handled in this contribution. For the aim to build a hybrid model with a higher prediction quality than the original FPM, we briefly highlight two open-source libraries: *FMI.jl* for integrating FMUs into the Julia programming environment, as well as an extension to this library called *FMIFlux.jl*, that allows for the integration of FMUs into a neural network topology to finally obtain a *NeuralFMU*.

Keywords NeuralFMU; FMU; Functional Mock-up Unit; NeuralODE; hybrid model; FMI; vehicle longitudinal dynamics model; PhysicsAI; scientific machine learning

1 Introduction

Hybrid modeling describes on the one hand the field of research in machine learning that focuses on the fusion of First Principle Models (FPMs), often in the form of symbolic differential equations, and machine learning structures like Artificial Neural Networks (ANNs). On the other hand, in the field of Ordinary Differential Equations (ODEs), *hybrid models* name the piece-wise concatenation of continuous models over time to obtain a discontinuous model, of which the numerically simulated solutions may not be continuously differentiable over time. In this article, we present a workflow concerning both interpretations of *hybrid modeling* by integrating custom, discontinuous simulation models and ANNs into a discontinuous NeuralFMU. For illustration, we use the example of learning a friction model for an industry typical automotive consumption simulation based on a Vehicle Longitudinal Dynamics Model (VLDM).

In the following, the term *hybrid model* is used to identify a model based on the combination of a FPM and Machine Learning (ML), whereas the concatenation of multiple continuous systems is referred to as *discontinuous model*.

1.1 State-of-the-art: Hybrid modeling

As part of research applications, the structural integration of physical models inside ML-topologies like ANNs is a topic growing attention. One approach for hybrid modeling is the integration of the FPM into the ML process by evaluating the forward propagation of the physical model as part of the loss function during training, namely Physics-informed Neural Networks (PINNs) [19]. In contrast, our method focuses on the structural integration of FPMs into the ANN/ODE itself and *not* only in the cost function, allowing much more flexibility with respect to what can be learned and influenced. However, it is also possible to build and train PINNs with the presented libraries. Another approach uses Bayesian Neural Stochastic Differential Equations (BNSDEs), which applies model selection together with Probably Approximately Correct (PAC) Bayesian bounds during the ANN training to improve hybrid model accuracy on basis of noisy prior knowledge [9]. Besides, Deep Auto-Regressive Networks (DARNs) can also be used to model physical systems. Similar to Recurrent Neural Networks (RNNs), the output of the last network inference is fed back into the neural network itself as input [7]. Different from RNNs, this feedback is not modeled as neural network state, but a simple feed-forward connection, and thus a DARN can be trained as conventional feed-forward network with all related simplifications and benefits. Finally, the combination of symbolic ODEs and object-orientated modeling languages like *Modia* is a promising and emerging research field too, because of the benefits of acausal modeling [3]. For a general overview on the growing field of hybrid modeling see e.g. [25] or [18].

With regards to learning system dynamics (the right-hand side of a differential equation), the structural integration of algorithmic numerical ODE-solvers into ANNs leads to significant improvements in performance, memory cost and numerical precision in comparison to the use of residual neural networks [4], while offering a new range of possibilities, e.g. fitting data observed at irregular time steps [11]. This integration of a numerical solver for ODEs into an ANN is known as *NeuralODE*, which is further introduced in Section 2.2. Probably the most mentioned point of criticism regarding NeuralODEs is the difficult transfer to real world applications for the following reasons:

- Real world models from common modeling tools are in general not available as symbolic ODEs;
- NeuralODE training tends to converge in local minima;
- NeuralODEs training often takes a considerable amount of calculation time.

Whereas the tendency to early converge to local minima and long training times can be tackled by different techniques (s. Sections 2.6 and 2.7), the major technical challenge that hinders hybrid modeling in industrial applications remains: FPMs are modeled and simulated inside closed tools. ML features, the foundation to allow for hybrid modeling, are missing in such tools and a seamless interoperability to ML-frameworks is not given. For example, to train the data-driven parts of hybrid models, determination of the loss function gradient through the ANNs and the FPMs themselves is needed. This requires different high-performance sensitivity algorithms like Automatic Differentiation (AD). ML-frameworks on the other hand, provide these abilities. To build high performing hybrid models, an interface between these two application worlds is needed.

1.2 Preliminary work: NeuralFMUs

In a preliminary publication [22], we started facing that issue and extended the concept of NeuralODEs by adding FPMs in the form of Functional Mock-up Units (FMUs) into this topology (s. Section 2.2). The resulting subclass of hybrid NeuralODEs, called *NeuralFMUs*, can be seen as the injection of system knowledge in the form of a FPM into the ANN model, equivalently the right-hand side of the ODE. This not only enhances the prediction quality, but also significantly reduces the amount of necessary training data, because *only* missing physical effects need to be learned. For example, the original FPMs were outperformed in terms of computational performance [23] and prediction accuracy [22], with trained only on data gathered by a single, short part of simulation trajectory. Further, the integration of a FPM can strongly enhance the extrapolation capabilities of the hybrid model compared to conventional pure data-driven models. In this article, we want to follow up these publications [22, 23] by providing a workflow and results not only for a synthetic example, but also a real world application in the form of an energy consumption simulation based on a VLDM. The following challenges, which are common in industrial applications but are often neglected for scientific experiments, are overcome as part of this publication: Discontinuity, closed-loop controllers inside of the system, an unknown system state and typical measurement errors (e.g. noise).

This article is further structured into three sections: A brief introduction to the used standards, methods, the corresponding software libraries *FMI.jl* and *FMIFlux.jl* and the VLDM. This is followed by the presentation of results of the example use case handling a NeuralFMU setup and training and finally closed by a conclusion with future outlook.

2 Materials and Methods

In this section, a short overview over the used standards, software and methods is given. On foundation of these, a workflow for the setup of NeuralFMUs in real applications is given and methods of initialization and training are elaborated. Finally, the VLDM, the FPM for the considered example use case, is introduced.

2.1 Functional Mock-up Interface (FMI)

The FMI standard¹ allows for the distribution and exchange of models in a standardized format independent of the modeling tool. The interface standard counts three version releases, the most popular version is 2.0 [14], the successor version 3.0 [15] was released in May 2022. An exported model container that fulfills the FMI requirements is called FMU. FMUs can be used in other simulation environments or even as part of entire Co-Simulations or System Structure and Parameterization (SSP) [16]. FMUs are subdivided into three major classes: Model Exchange (ME), Co-Simulation (CS) and new in FMI 3.0 Scheduled Execution (SE). The possible use cases depend on the FMU-type and the availability of standardized and optionally implemented FMI functions. Most relevant for the considered use case are ME-FMUs, because this type allows for manipulation and extension of system dynamics before the numerical integration.

To optimize simulation performance, fast physical effects like the change from stick- to slide-friction or the firing of an electrical diode are often modeled in a discontinuous way. This means that the expressions of the right-hand side of the ODE model may change depending on the current system state and time, whereas this transition is discrete. Inside FMI, this means ME-FMUs may contain state- or time-dependent discontinuities, which are triggering so called *events*. The actual event time point, the instant at which the equations and/or the state of the model is modified, is defined by a predefined time point itself (time-events) or the zero-crossing of a scalar value (state-events), also called the *event indicator*. For a detailed view on the event definition and handling, see [15]. Basically, any ME-FMU with continuous state x_c , discrete state x_d and time- and/or state-events can be seen as a hybrid ODE, as in Figure 1. Continuous states may change in time, while discrete states can only change their value at event instances.

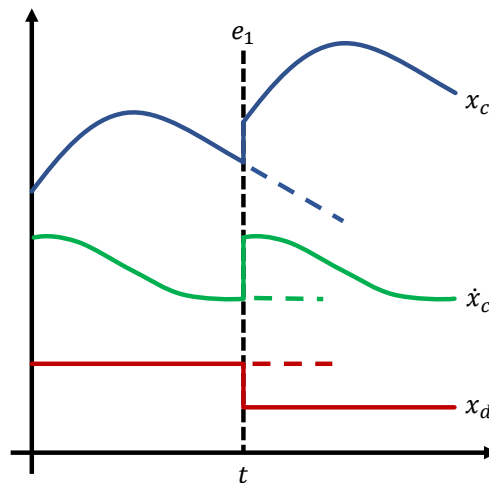


Figure 1: Exemplified simulation of a ME-FMU with events (hybrid ODE). The single (piecewise) continuous system state x_c (blue) and state derivative \dot{x}_c may depend on a discrete system state x_d (red), which is unknown in general for FMUs. Not handling events like e_1 (black-dashed), leads to wrong system values (blue-, green-, red-dashed), because the system state is not updated properly.

¹<https://fmi-standard.org/>

2.2 NeuralODEs & NeuralFMUs

NeuralODEs are defined by the structural combination of an ANN and a numerical ODE-solver, see figure 2. As a result, the ANN acts as the right-hand side of an ODE, whereas solving of this ODE is performed by a conventional ODE-solver. If external requirements (tolerance or stiffness) change, the ODE-solver can be easily replaced by another one. The scientific contribution at this point is not only the idea of this subdivision, but also, more importantly, a concept to allow training this topology on a target solution for the ODE. This requires propagation of the parameter sensitivities of the ANN through the ODE-solver [4]. *DiffEqFlux.jl*² is already available as a ready-to-use library for building and training NeuralODEs in the Julia programming language [17].

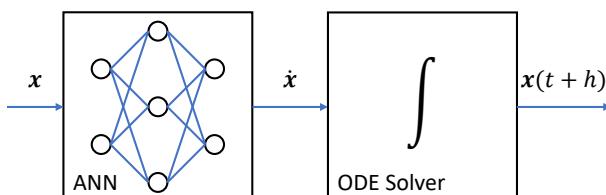


Figure 2: Topology of a NeuralODE consisting of a feed-forward ANN and a numerical ODE-solver: The current system state \mathbf{x} is passed to the ANN, based on that the state derivative $\dot{\mathbf{x}}$ is calculated and integrated into the next system state $\mathbf{x}(t+h)$ by the ODE-solver with time step size h .

We extend the concept of NeuralODEs by one or more FPMs in the form of FMUs to obtain a class of hybrid models, named *NeuralFMUs* [22]. Using the example of a ME-NeuralFMU, the ME-FMU replaces the ANN of the NeuralODE, because it calculates the system dynamics $\dot{\mathbf{x}}$ based on the current system state \mathbf{x} . To optimize the system state, an additional (state) ANN can be placed *before*, and to manipulate the system dynamics, an additional (derivative) ANN can be placed *after* the FMU. This exemplified structure of a NeuralFMU is given in Figure 3. However, the concept of

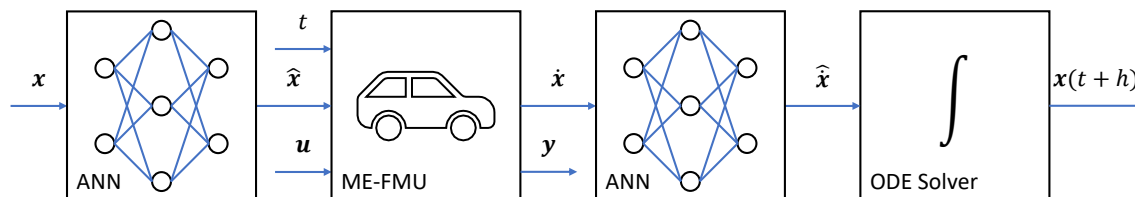


Figure 3: Topology of a ME-NeuralFMU (example) consisting of two feed-forward ANNs, a ME-FMU and a numerical ODE solver: The current system state \mathbf{x} is passed to a (state) ANN, based on that a manipulated system state $\hat{\mathbf{x}}$ is calculated and passed to the ME-FMU. There, the system state derivative $\dot{\mathbf{x}}$ is computed and manipulated by another (derivative) ANN into the changed system state derivative $\hat{\dot{\mathbf{x}}}$, which is finally integrated into the next system state $\mathbf{x}(t+h)$ by the ODE-solver with time step size h . Also the FMU's input \mathbf{u} , output \mathbf{y} or parameters (not shown) could be connected to the ANNs.

NeuralFMUs itself is very generic and does not restrict the positions or number of FMUs inside the ANNs or limits which signals are manipulated by the ANNs. Inference of a NeuralFMU can be achieved by evaluating each of the considered blocks one after another. Whereas inference of the derivative ANN (between FMU and solver) is straight forward, because the system dynamics are passed as input to the ANN, inference of the state ANN needs additional attention. In case of an event inside the FMU, the FMU system state $\hat{\mathbf{x}}$ may be changed during event-handling. This new state must be propagated backwards through the state ANN to calculate a new system state \mathbf{x} for the ODE solver to reinitialize the numerical integration at. Because ANNs are not invertible by default, the new state \mathbf{x} must be determined by solving an optimization problem. In case of a state event, the required accuracy for the optimization solution is high, because solving for a state that is slightly before the event instance will trigger the event again. To prevent this, the optimization objective can be defined not only on hitting the FMU state $\hat{\mathbf{x}}$, but also on the change of the sign of the corresponding event indicator. This enhanced objective promotes finding a state that lays after the event instance in time. In case of time events, high accuracy for the optimization result is desirable but not required.

²<https://github.com/SciML/DiffEqFlux.jl>

For a more detailed view on the concept of NeuralFMUs and the technical training process, see [22]. In the following, only ME-NeuralFMUs are considered and identified by the short term *NeuralFMU*.

2.3 Software

Combining and training physical and data-driven models inside a single industry tool is currently not possible, therefore, it is required to transfer FPMs to a more suitable environment. After the export from modeling environment and import into the ML environment, the first-principle is extended to a hybrid model. Finally after succeeded training, it is necessary to re-import the hybrid model back into the original modeling environment, for further modeling or the setup of larger system co-simulations. For the considered importing and exporting between environments, an industry typical model exchange format is needed. Because the FMI is an open standard and widely used in industry as well as in research applications, it is a suitable candidate for this aim. On the side of modeling environments, FMI is already implemented in many common tools, but a software interface that integrates FMI into the ML environment is still needed (s. Section 2.3.2).

2.3.1 Julia Programming Language

In this section, it is shortly explained why the authors picked the Julia programming language (from here on simply referred to as *Julia*) for the presented task as ML environment. Julia is a dynamic typing language developing since 2009 and first published in 2012 [1], with the aim to provide fast numerical computations in a platform-independent, high level programming language [2]. The language and interpreter was originally invented at the *Massachusetts Institute of Technology*, but till today many other universities and research facilities have joined the development of language expansions, which mirrors in many contributions from different countries and even in its own conference, the *JuliaCon*³. Besides many great libraries in the field of scientific machine learning, there are multiple libraries for AD like e.g. *ForwardDiff.jl*⁴ [20] and *Zygote.jl*⁵ [10]. Further, different modeling related libraries are available, like for example *Modia.jl*⁶ [6], which allows for object-orientated white-box modeling of mechanical and electrical systems, syntactically similar to *Modelica*[®], in Julia.

2.3.2 FMI in Julia: *FMI.jl*

The Julia library *FMI.jl* provides high level commands to unzip, allocate, parameterize and simulate entire FMUs, as well as plotting the solution and parsing model meta data from the model description. Because FMI has already three released specification versions and is under ongoing development, one major goal of *FMI.jl* is to provide the ability to simulate different version FMUs with the same user front-end. To satisfy users who prefer close-to-specification programming, as well as users that are new to the topic and favor a smaller but more high level command set, we provide high level Julia commands, but also the possibility to use the more low level commands specified in the FMI standards [14, 15]. The library and its feature set are constantly growing.

2.3.3 NeuralFMUs in Julia: *FMIFlux.jl*

The open-source library *FMIFlux.jl* extends *FMI.jl* and allows for the fusion of a FMU and an ANN. As in many other machine learning frameworks, a deep ANN in Julia using *Flux.jl*⁷ is configured by chaining multiple neural layers together. Probably the most intuitive way of integrating a FMU into this topology, is to simply handle the FMU as a network layer. In general, *FMIFlux.jl* does not make restrictions to:

- which FMU signals can be used as layer inputs and outputs. It is possible to use any variable that can be set via `fmi2SetReal` or `fmi2SetContinuousStates` as input and any variable that can be obtained by `fmi2GetReal` or `fmi2GetDerivatives` as output;
- where to place FMUs inside the ANN topology, as long as all signals are traceable via AD (no signal cuts).

Dependent on the FMU type, ME, CS or SE, different setups for NeuralFMUs should be considered. In this article, only ME-NeuralFMUs are highlighted.

³<http://www.juliacon.org>

⁴<https://github.com/JuliaDiff/ForwardDiff.jl>

⁵<https://github.com/FluxML/Zygote.jl>

⁶<https://github.com/ModiaSim/Modia.jl>

⁷<https://fluxml.ai/Flux.jl/stable/>

2.4 Workflow

On the foundation of Julia, FMI, *FMI.jl* and *FMIFlux.jl*, we suggest the following workflow for designing custom NeuralFMUs:

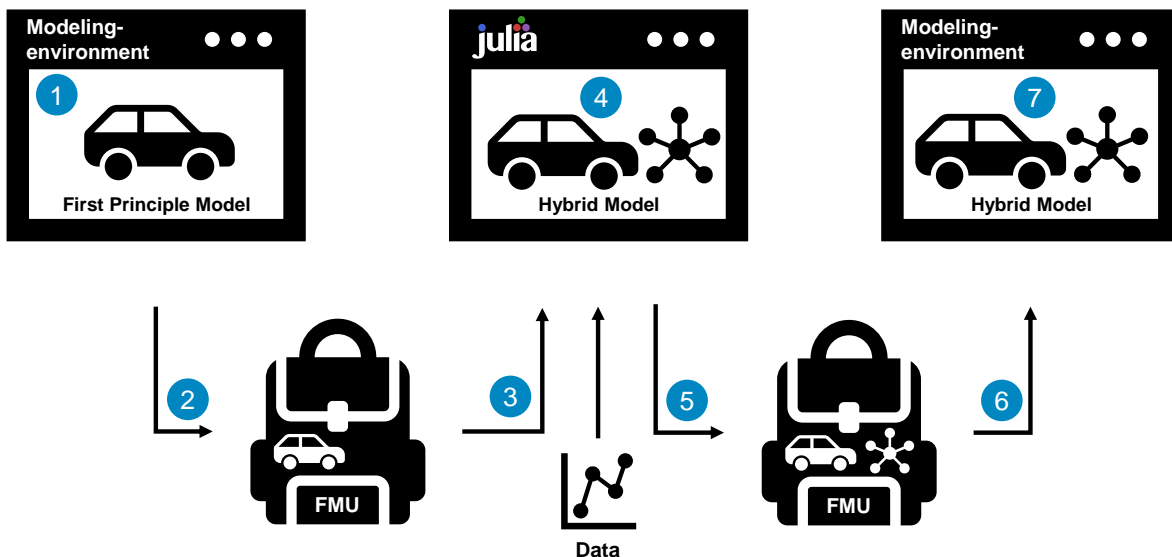


Figure 4: Workflow of the presented hybrid modeling application using a modeling tool supporting FMI (export and import) and *FMI.jl* together with *FMIFlux.jl*.

The presented development process of a NeuralODE/FMU in Figure 4 covers the following steps:

1. The FPM is designed by a domain expert inside of a familiar modeling tool supporting FMI (export and import).
2. After modeling, the FPM is exported as FMU.
3. The FPM-FMU is imported into Julia using *FMI.jl*.
4. The FPM is extended to a hybrid model and trained on data, for example of a real system or a high-resolution and high-fidelity simulation, using *FMIFlux.jl*.
5. The trained hybrid model is exported as FMU using *FMI.jl*.
6. The hybrid model FMU is imported into the original modeling environment.
7. The improved hybrid model FMU can further be used in different modeling and simulation tools (including the original tool the FPM was exported from).

2.5 Data pre- and post-processing

In many ML applications, pre- and post-processing are not only instrumental, but necessary. For training conventional ANNs, pre-processing of training data can often be performed for one single time, before batching and the actual training. For NeuralFMUs, the FMUs may generate outputs within a range that is excessively saturated by the activation functions inside the ANN. Further, the FMUs may expect inputs within a range not generatable by the ANN, because of the limited output of the activation functions. Therefore, all signals must be processed at the interfaces between the FMUs and ANNs. If no expert knowledge of the data range of the FMU inputs and outputs is available, a good starting point can be to scale and shift data into a standard normal distribution. Because the FMU output and input may shrink or grow during training because of new state exploration by the changed dynamics, scaling and shifting parameters should be parts of the optimization parameters during training. See Section 3.2 for a visual example topology using data pre- and post-processing around an ANN.

2.6 Initialization (Pre-training)

Obtaining a trainable (solvable) NeuralFMU is not trivial. Using larger or complex FMUs together with randomly initialized ANNs often leads to instable and/or stiff ODE-system. Whereas starting the training process with an unnecessary stiff NeuralFMU (more stiff than the final solution) leads to long training times, an instable system might not be trainable at all. Without further investigation, selecting random initialized ANNs as part of NeuralFMUs often lead to hardly trainable systems in different use cases like e.g. a controlled EC-Motor Hardware in the Loop (HiL)-simulation, a thermodynamic cabin simulation or in modeling the human cardiovascular system [23]. Therefore, we suggest three different initialization strategies for ANNs inside of NeuralFMUs: Neutral Initialization Pre-Training (NIPT), Collocation Pre-Training (CCPT) and the introduction of a FPM/ANN gates topology. A major advantage of all initialization modes is, that sensitivities during the initialization process don't need to be propagated through the ODE solver (the actual ODE is not solved), therefore, the computational effort is much less, compared to the actual training described in Section 2.7.

For a better understanding, initialization strategies are not exemplified at a NeuralFMU as in Figure 3, but a suitable NeuralFMU topology for this use case, which includes only one FMU, one ANN (derivative) and the numerical solver. The concepts can be easily modified to fit other topologies.

2.6.1 Neutral Initialization Pre-Training (NIPT)

If the system state derivative is not known, cannot be measured and/or can hardly be approximated, NIPT of the ANNs can deliver a good initialization for the ANN parameters for the later training. Similar to auto-encoder networks, the aim is to train the ANN so, that the output equals the input for a set of training data, see Figure 5. Different from auto-encoders, the hidden network layers don't need to narrow in width. The training result is, that the solution of the initialized NeuralFMU converges against the solution of the FMU itself - or if multiple FMUs are present - the solution of the chained FMU-system without ANNs. If the FMU solution is already close to the target solution (the term *close* strongly depends on the system constitution), this might be a suitable initialization method. Only for training data acquisition, it is necessary to perform a single forward simulation. For the actual training, solving the ODE system is not required.

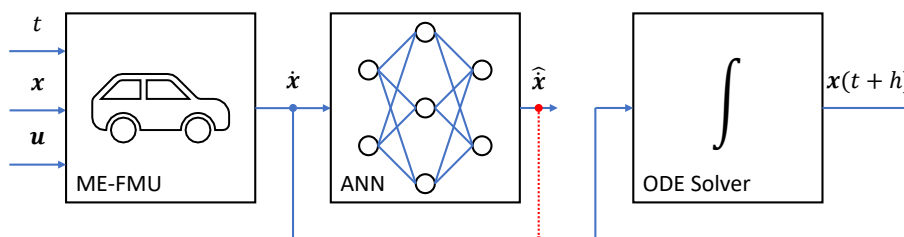


Figure 5: For NIPT, a single reference simulation with unchanged \dot{x} is performed to calculate the ANN output $\hat{\dot{x}}(t)$ for every system state $x(t)$. Based on that, the actual training can be performed. As soon as the training goal $\dot{x} \approx \hat{\dot{x}}$ (red-dotted) is reached, the NeuralFMU dynamics equals the dynamics of the FMU itself, which results in the same solution for both. In this case, the ANN behaves *neutral*.

2.6.2 Collocation Pre-Training (CCPT)

Similar to the collocation training of NeuralODEs [21], collocation training can be performed for NeuralFMUs, too. The CCPT is similar to NIPT, the major difference is the training goal, see Figure 6. Whereas NIPT focuses on propagating the derivatives unchanged through the ANN, CCPT aims on hitting the derivatives of the ODE-solution, so that after integration (solving), the target solution can be obtained.

This method needs knowledge of the entire system state trajectory $\tilde{x}(t)$ as well as the (at least approximated) state derivative $\tilde{\dot{x}}(t)$. In general, only a part of the system state and/or derivative of a real system can be measured. Different methods allow for estimating the unknown states like e.g. Kalman-filter [12]. To converge against the target solution, CCPT needs high-quality data of the system state and derivative. Derivatives could be approximated by finite differences or filters, see [21] for an overview. Note that approximating the derivatives may decrease the quality of the pre-training process.

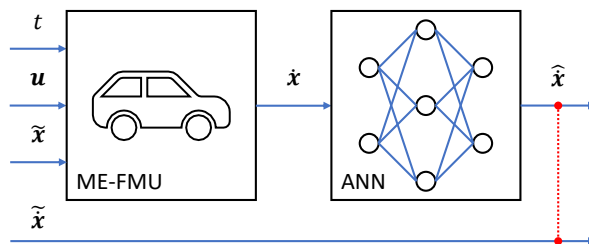


Figure 6: For CCPT, no reference simulation is performed. For a given state trajectory $\tilde{x}(t)$ (e.g. from data), every state is propagated through the FMU and the ANN. As soon as the training goal $\hat{x} \approx \tilde{x}$ (red-dotted) is reached, the NeuralFMU dynamics equals the target dynamics \tilde{x} (e.g. from data). As a result, the later NeuralFMU solution matches the given state trajectory for a perfect known \tilde{x} . The target dynamics \tilde{x} may be estimated by deriving and filtering the given system state $\tilde{x}(t)$ or might be known from measurements.

CCPT is only usable, if the states of the training objective matching the state derivatives manipulated by the ANN. Whereas this is often the case in academic examples, in real applications it is not, which is further exemplified at the VLDM in Section 3.2.

To summarize, NIPT doesn't require the entire state, but converges only against the FMU solution. CCPT on the other hand, converges against a given target solution, but requires a known target solution and derivative.

2.6.3 FPM/ANN gates

The challenge of finding a good initialization by a foregoing pre-training procedure can be bypassed by introducing a slightly modified topology, that literally introduces a bypass around the ANN, see Figure 7.

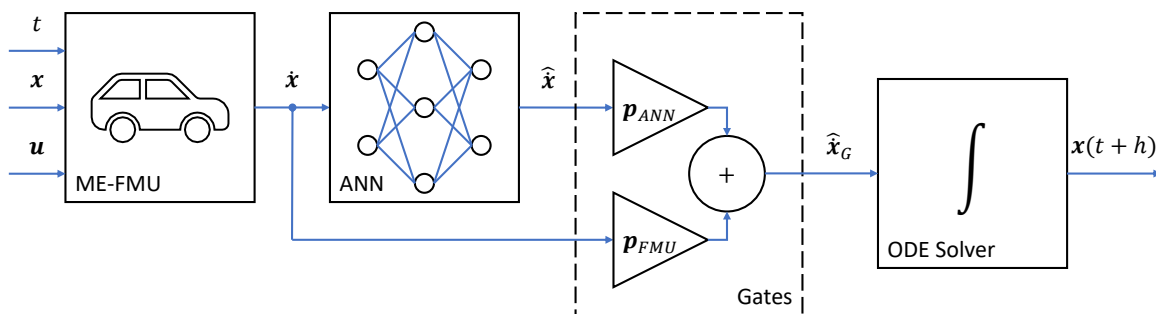


Figure 7: ME-NeuralFMU with FPM/ANN gates: The ME-FMU receives the current time t and state x from the numerical ODE solver together with an external input u and computes the corresponding state derivative \dot{x} . Two gates p_{ANN} and p_{FMU} scale how much dynamic changes by the ANN and the FMU are introduced to the derivative vector \hat{x}_G . Finally, the derivative vector \hat{x}_G is passed to the ODE solver with (adaptive) step size h and integrated to the next system state $x(t+h)$.

As in Figure 7, the system state derivative \hat{x}_G is defined as follows, where \circ stands for the Hadamard-product:

$$\hat{x}_G = p_{ANN} \circ \hat{x} + p_{FMU} \circ \dot{x} \quad (1)$$

On the one hand, for the case $p_{ANN} = 0$ and $p_{FMU} = 1$, the resulting simulation trajectory is just the simulation trajectory of the original FMU, independent of the ANN parameters. In this way, the NeuralFMU can be initialized without a special initialization routine, while also being capable of manipulating the system dynamics if the parameter p_{ANN} is changed to a non-zero value. On the other hand, for the case $p_{ANN} = 1$ and $p_{FMU} = 0$, only the ANN affects the state dynamics and the original FMU dynamics are used only as input for the ANN. The parameters p_{ANN} and p_{FMU} can be optimized along the other training parameters, or dependent on the use case, with a static or dynamic decay/increase. As a final note, CCPT and the FPM/ANN gates topology doesn't exclude each other and can be used together on a NeuralFMU initialization.

2.7 Batching & Training

The training is not performed on the entire data trajectory at one time (e.g. the used CADC (Road) is 1001.22 s long). Instead the trajectory is batched. The major challenge at this point is that for a given batch element start time $t \neq t_0$, often only the continuous part of the model state vector $\mathbf{x}_c(t)$ of the ME-FMU is known. In general, the discrete part $\mathbf{x}_d(t)$ is unknown. As a result, if not explicitly given, a suitable discrete state is determined during the initialization procedure inside the FMU, but it is not guaranteed that this state matches the data and/or expectations. This circumstance also applies to the determination of the initial value of the discrete states $\mathbf{t}_{0,d}$, but measurements are often started in a stationary state, where a good understanding of the correct discrete states is given, even if they are not explicitly parts of the data measurements.

As a consequence, training cannot be initialized at an arbitrary element of the batch (time instant) because of the unknown discrete states, which might be initialized unexpected if ignored. Estimating the discrete system state on basis of data is not trivial and may need significant expert knowledge about the model itself. So, a straight-forward strategy to handle this is to simulate all batches in the correct order without resetting the FMU between batch elements. Although this does not guarantee the correct discrete state when switching from one batch element to the next during training, the discrete solution converges against the target together with the continuous solution.

Another option is to simulate the entire trajectory for one single time and making memory copies of the entire FMU state using e.g. `fmi2GetFMUstate` (in FMI 2.0) at the very beginning of every batch element. This allows for random batches, which might improve the training success and speed. Because the feature required to save and load the FMU memory footprint is optional in FMI and thus often not implemented, this strategy is not further highlighted at this point, but can be implemented in a straight-forward manner.

Besides the ones mentioned, many techniques for NeuralODEs can be adapted to improve the training process in terms of stability and convergence, like for example *multiple shooting* as in [24], because NeuralFMUs are a subclass of NeuralODEs.

3 Results

The considered method is validated at the following application: Based on the introduced VLDM, a hybrid model is deployed leading to a significant better consumption prediction than the original FPM. Even if the FPM already considers multiple friction effects, it is assumed that the prediction error is the result of a wrongly parameterized or an additional, non-modeled friction effect. The goal is to inject an additional vehicle acceleration to force the driver controller to perform a higher engine torque, and thus to increase the vehicle energy consumption.

3.1 Example Model: Vehicle Longitudinal Dynamics Model (VLDM)

In this section, the used FMU model is introduced: The model represents the longitudinal dynamics of an electric *Smart EQ fortwo* and is an adaption from a model of the *Technical University of Munich* [5]. In automotive applications, longitudinal dynamics models are often used to simulate energy consumption, thus only related effects are represented in the model. The original model was created in MATLAB®/Simulink®, replicated analogously in the modeling language Modelica® and exported as FMU. The following Figure 8 shows the topology of the simulation model. The full vehicle model is modular and consists of six core components [8].

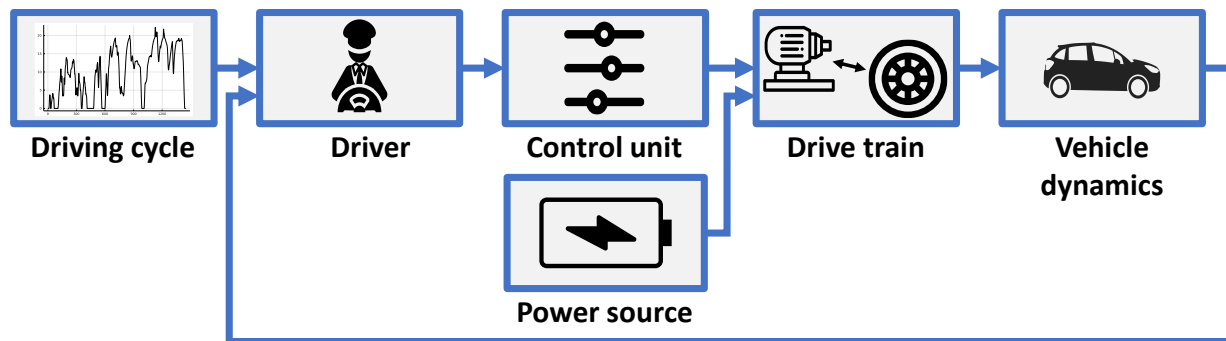


Figure 8: Topology of the VLDM (own representation adapted from [5]).

The top-layer components of the vehicle are the *Driving cycle*, the *Driver*, the *Control unit*, the *Power source*, the *Drive train* and the *Vehicle dynamics* subsystem. The target vehicle speed, read from a driving cycle tabular in the *Driving cycle* subsystem, is forwarded to the *Driver*. The *Driver* consists of two PI-controllers for the acceleration and brake pedal, controlling the vehicle to follow the given driving cycle. The block *Control unit* calculates the desired torque from the pedal position. The required power is provided by the *Power source* component, modeling the vehicle battery. In the *Drive train* block, the sources of acceleration and braking torques are implemented. This component contains the electric motor, the power electronics, the transmission and the tire model. In the component *Vehicle dynamics*, the rolling-, air- and slope-resistance are implemented. The resulting force and torque determine the acceleration of the vehicle, and after numerical integration the speed and position [5]. Finally, the vehicle speed is fed back into the *Driver* subsystem and closes the controller loop. Together with the model itself, multiple measurements from an automotive driving test rig with different driving cycles like the Common Artemis Driving Cycles (CADC), New European Driving Cycle (NEDC) and Worldwide harmonized Light-duty vehicles Test Cycle (WLTC) where published⁸. We use the driving cycles CADC (Road) and WLTC (class 2) for the presented experiment.

The simulation model counts six continuous states x_c in total:

- x_1 the PI-controller state (integrated error) for the throttle pedal (*Driver*);
- x_2 the PI-controller state (integrated error) for the brake pedal (*Driver*);
- x_3 the integrated driving cycle speed, the cycle position (*Driving cycle*);
- x_4 the vehicle position (*Vehicle dynamics*);
- x_5 the vehicle velocity (*Vehicle dynamics*);
- x_6 the cumulative consumption (energy).

In analogy, the six continuous state derivatives \dot{x}_c are:

- \dot{x}_1 the PI-controller error/deviation for the throttle pedal (*Driver*);
- \dot{x}_2 the PI-controller error/deviation for the brake pedal (*Driver*);
- \dot{x}_3 the driving cycle speed (*Driving cycle*);
- \dot{x}_4 the vehicle velocity (*Vehicle dynamics*);
- \dot{x}_5 the vehicle acceleration (*Vehicle dynamics*);
- \dot{x}_6 the current consumption (power).

Note that this system features different challenging attributes, like:

- The system is highly discontinuous, meaning it has a significant amount of explicitly time-dependent events (100 events per second). This further limits the maximum time step size for the numerical solver and so worsens the simulation and training performance;
- The simulation contains a closed-loop over multiple subsystems with two controllers running at 100 Hz (the source of the high-frequent time-events);
- The system contains a large amount of state-dependent events, triggered by 22 event-indicators;
- Measurements of the real system are not equidistant in time (even if it was saved this way, which introduces a typical measurement error);
- Only a subpart of the system state vector is part of measurements, the remaining parts are estimated;
- Measurements are not exact and contain typical, sensor- and filter-specific errors (like noise and oscillation);
- There is a hysteresis loop for the activation of the throttle and brake pedal, the PI-controller states are initialized at corresponding edges in the hysteresis loop;
- The system is highly non-linear, e.g. multiple quantities are saturated;
- Characteristic maps (data models) for the electric power, inverted electric power and the electric power losses are used.

Combining all these attributes results in a challenging FPM for the considered hybrid modeling use case.

⁸https://github.com/TUMFTM/Component_Library_for_Full_Vehicle_Simulations

3.2 Topology

Combining the original NeuralFMU topology (s. Figure 3) with pre- and post-processing (s. Section 2.5) and FPM/ANN gates (s. Section 2.6.3) results in the topology as shown in Figure 9, which is used for training the hybrid model in the considered use case. In general, understanding at least some aspects of the physical effect, which is to be modeled by the

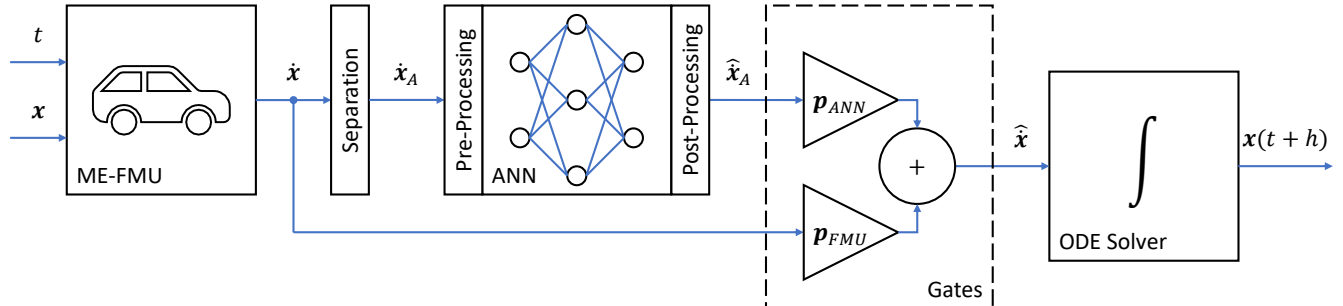


Figure 9: Topology of the used ME-NeuralFMU: The ME-FMU receives the current time t and state \mathbf{x} from the numerical ODE solver and computes the corresponding state derivative $\dot{\mathbf{x}}$. The state derivative is then trimmed to a subset of derivatives $\dot{\mathbf{x}}_A$. Before the ANN transforms $\dot{\mathbf{x}}_A$, the signals are pre-processed to approximately fit a standard normal distribution. After the ANN inference, the inverse transformation of the pre-process is applied in the post-processed and $\hat{\mathbf{x}}_A$ is obtained. Two gates \mathbf{p}_{ANN} and \mathbf{p}_{FMU} scale how much $\hat{\mathbf{x}}_A$ and $\dot{\mathbf{x}}$ are introduced to the final derivative vector $\hat{\mathbf{x}}$. Finally, the changed derivative vector $\hat{\mathbf{x}}$ is passed to the ODE solver with (adaptive) step size h and integrated to the next system state $\mathbf{x}(t+h)$. The used FMU has no continuous inputs \mathbf{u} , the driving cycle is part of the model and depends only on the time t .

ANNs, is a great advantage. Basically, any value of the FMU that is accessible via the FMI can be used as input for the ANNs: The system states and -derivatives, system inputs as well as any other system variable (or output) that depends on the system state, input and/or time. This allows for a wide variety of NeuralFMU topologies. However, using all available variables in the interface to the ANNs can result in sub-optimal training performance, because more variable sensitivities need to be determined and signals without physical dependency could be misinterpreted as dependent. This motivates the use of a clever, minimal subset of the available FMU variables. Often, state and state derivatives are good choices for variables to feed into the ANN, because from a mathematical point of view, the system state holds all relevant information in a minimal representation. Nevertheless, adding additional variables may be productive, even if the encapsulated system information is redundant, if the correlations between these variables and the training objective is easier to fit for an ANN compared to the correlation with system states and/or derivatives.

For the considered use case, a friction-effect is learned. Conventional mechanical friction models, like viscous damping or slip-stick-friction, often depend on the physical body's translational or rotational velocity. Therefore, especially the vehicle speed should be considered. Further, the current vehicle acceleration and power is also given as inputs to the ANN. The training objective is to match the cumulative consumption from training data by manipulating the vehicle acceleration. Here, CCPT can't be used, because the CCPT objective would be to fit the cumulative consumption derivative, so the current consumption, but this value is not affected by the ANN.

To summarize, the following variables (compare to Figure 9) are used:

- $\dot{\mathbf{x}}_A = \{\dot{x}_4, \dot{x}_5, \dot{x}_6\}$ corresponds to the vehicle speed, acceleration and power (current consumption). These are the inputs for the ANN;
- $\hat{\mathbf{x}}_A = \{0, 0, 0, 0, \hat{x}_5, 0\}$ corresponds to the estimated vehicle acceleration by the ANN. This is the output of the ANN (technically, it is the only output, because the other five dynamics are assumed always zero and are neglected);
- $\mathbf{p}_{ANN} = \{0, 0, 0, 0, p_1, 0\}$, only the influence of the vehicle acceleration from the ANN can be controlled via p_1 (this is the only ANN output);
- $\mathbf{p}_{FMU} = \{1, 1, 1, 1, p_2, 1\}$, only the influence of the vehicle acceleration from the FMU can be controlled via p_2 (all other derivatives contribute by 100%).

Please note that if the considered effect could depend on the system states, states could also be passed as input to the ANN. Because the hybrid model reuses the FPM and therefore the ANN only needs to approximate the unmodeled

physical effect, a very light-weight net layout is sufficient, as shown in Table 1. This results in a fast training because of the small number of parameters.

Table 1: ANN layout and parameters of the used topology.

Index	Type	Activation	Inputs	Outputs	Bias	Parameters
1	Pre-process	none	3	3	0	6
2	Dense	tanh	3	32	32	128
3	Dense	tanh	32	1	1	33
4	Post-process	none	1	1	0	0
5	Gates	none	1	1	0	2
						Sum: 169

3.3 Consumption prediction

3.3.1 Training

After training on a batch with a batch element length of 100 s, resulting in 11 batch elements, and 18 epochs on the CADC (Road), the NeuralFMU is able to outperform the FPM on training data, see Figures 10, 11 and 12. The following figures show the predicted cumulative consumption over time of the original FPM, compared to the trained NeuralFMU. Training is not converged at this point. The cost function is implemented as ordinary Mean Squared Error (MSE) between data and predicted cumulative consumption. For parameter optimization *Adam* [13] together with an exponential decay⁹ is used. The training is performed single-core on CPU¹⁰ and takes ≈ 5 hours. During interpretation of results, please note the small amount of data used for training: A single driving cycle measurement trajectory (mean over two real experiments).

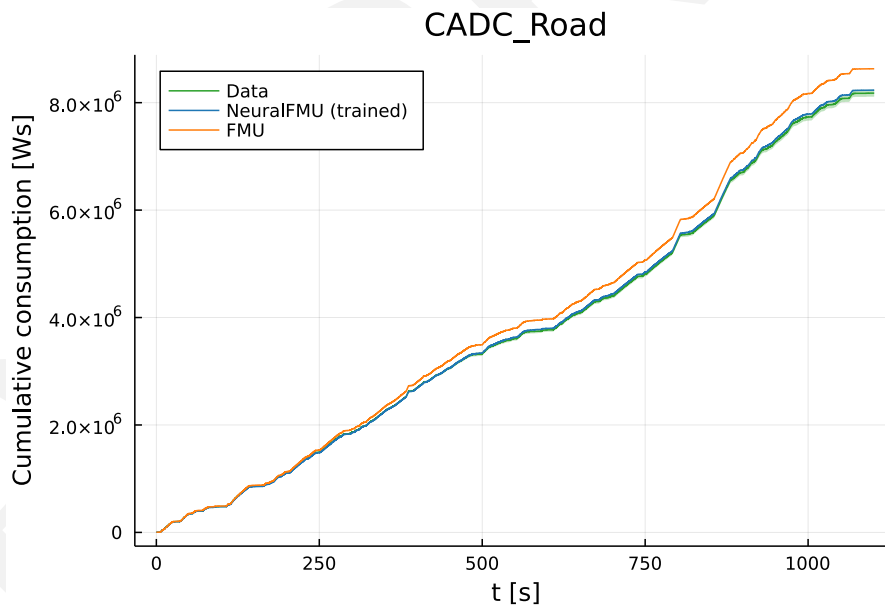


Figure 10: Cumulative consumption prediction on the CADC (Road), that is part of training data. The NeuralFMU (blue) lays almost on the training data mean (green) and inside the data uncertainty region (green, translucent). On the other hand, the simulation results of the original FPM as FMU (orange) slowly drifts out the data uncertainty region, resulting in a relative large error at the simulation stop time compared to the NeuralFMU.

⁹Initial step size: $1e-3$, Decay (new step size multiplier): 0.95 every step, Min. step size: $1e-5$.

¹⁰Intel® Core™ i7-8565U on Windows 10 Enterprise 20H2

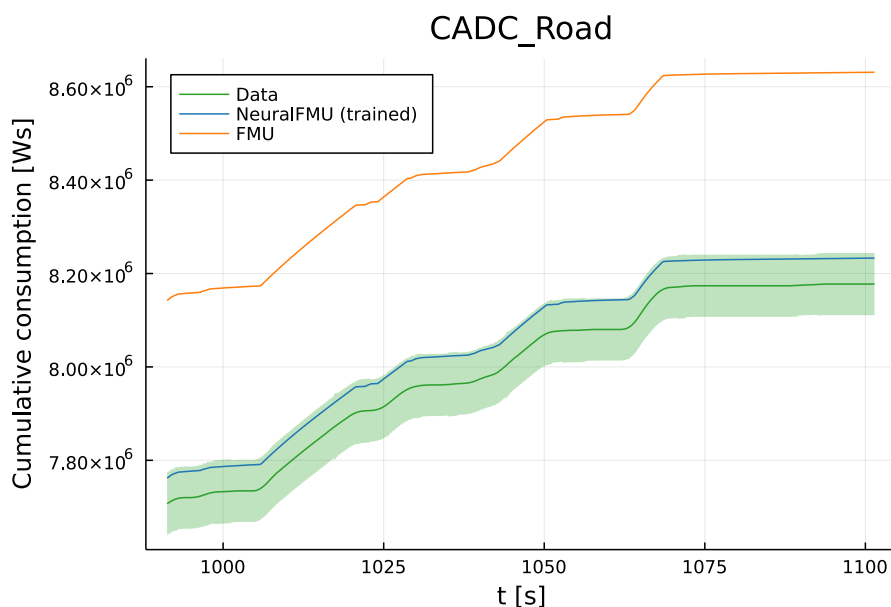


Figure 11: Deviation on the last 10% of the cumulative consumption prediction on the CADC (Road), that is part of training data. The final consumption prediction accuracy of the NeuralFMU (blue) significantly increases compared to the original FMU (orange), lays inside the measurement uncertainty (green, translucent) and close to the data mean (green). The original FPM prediction lays completely outside of the measurement uncertainty.

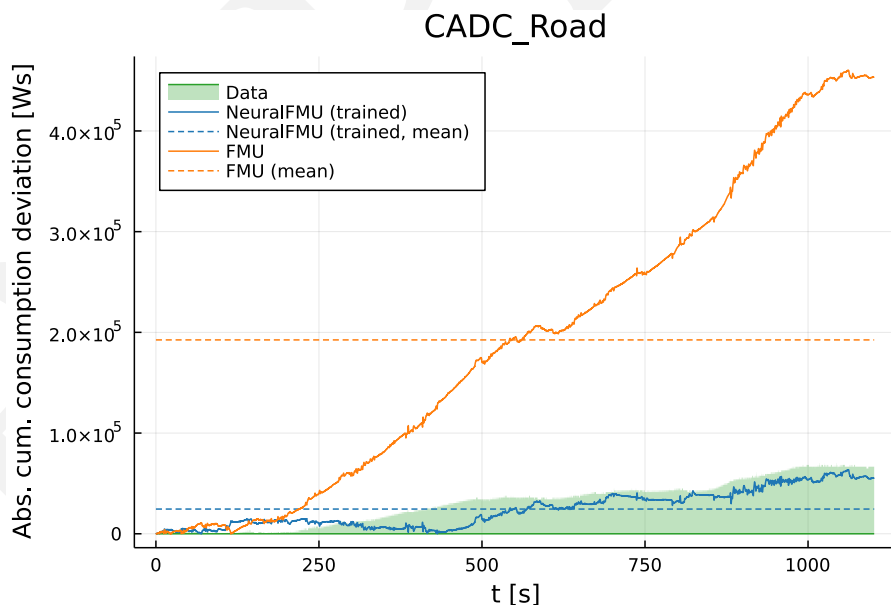


Figure 12: Deviation (absolute error) of the consumption prediction between data and the NeuralFMU (blue) compared to the original FPM as FMU (orange) on the CADC (Road), that was part of training data. After ≈ 300 s, the NeuralFMU solution lays inside the data uncertainty region (green, translucent) and outperforms the FPM in terms of prediction accuracy. Further, the NeuralFMU error is at any time step significantly smaller than the mean error of the FMU (orange, dashed).

3.3.2 Testing (Validation)

After training, the NeuralFMU is validated against unknown data by simulating another driving cycle, the WLTC (class 2), that is not known from training. Results and explanations can be seen in Figures 13, 14 and 15.

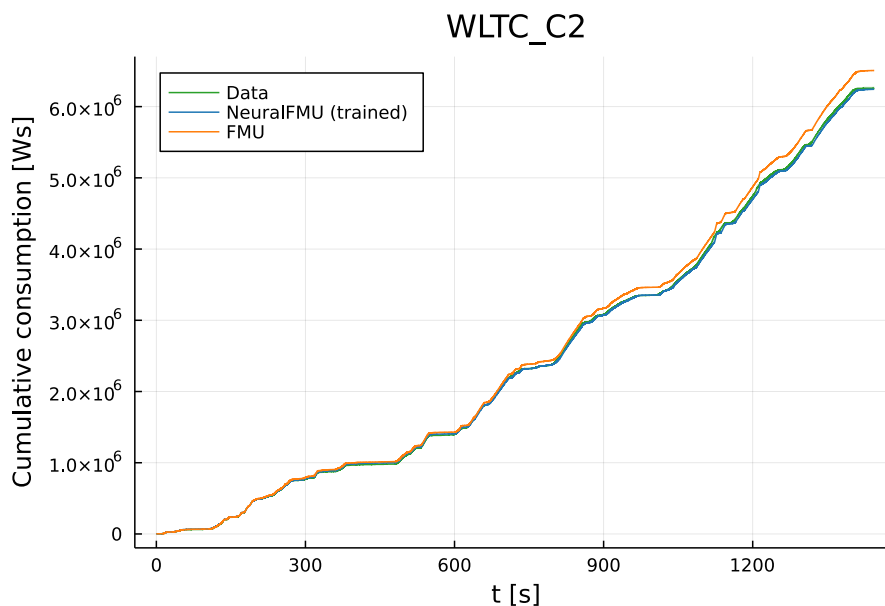


Figure 13: Comparison of the cumulative consumption prediction, using the WLTC (class 2), that is not part of the NeuralFMU training data. As for training data, the NeuralFMU prediction (blue) is closer to the measurement data mean (green), compared to the original FPM prediction (orange).

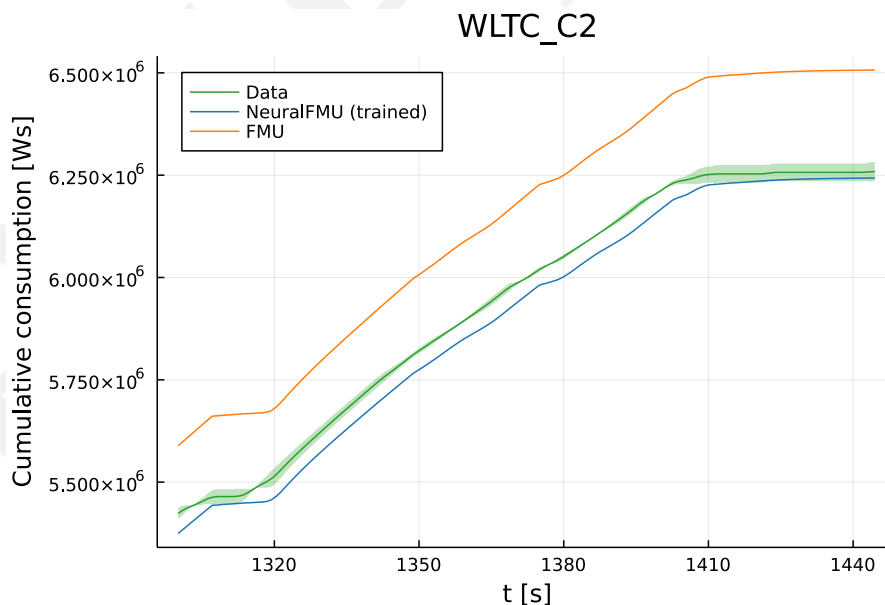


Figure 14: Deviation on the last 10 % of the simulation trajectory of the NeuralFMU (blue) compared to the original FPM as FMU (orange) and experimental data mean (green). The unknown WLTC (class 2) is used for testing. The NeuralFMU prediction is much closer to the data mean than the original FPM and predicts a final value inside of the measurement uncertainty.

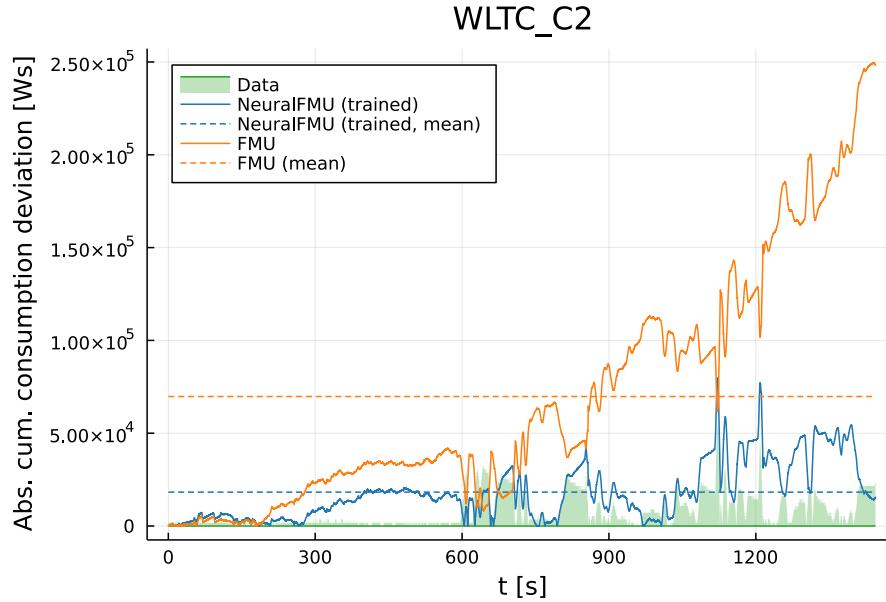


Figure 15: Absolute error of the consumption prediction of the NeuralFMU (blue) compared to the original FPM as FMU (orange). The unknown WLTC (class 2) is used for testing. Even if the NeuralFMU solution (blue) does not always lay inside the data uncertainty region (green), it leads to a much better prediction compared to the original FPM, that in contrast almost completely misses the data uncertainty area (green, translucent).

For training as well as for testing data, the NeuralFMU solution leads to a smaller MSE, maximum error and final error than the solution of the original FPM. For the training cycle the NeuralFMU solution proceeds inside of the measurement uncertainty, which is a great success. Also for testing data, the NeuralFMU increases prediction accuracy compared to the FPM, but leaves the data uncertainty region in some sections. A detailed overview of the training and testing results can be seen in Table 2. Because longitudinal dynamics models are often used to predict the cumulative

Table 2: Training and testing results with solver *Tsit5* after 18 training epochs. Errors are calculated against the data mean of two chassis dynamometer runs.

Model	Cycle	MSE [W^2s^2]	max. error [Ws]	final error [Ws]	sim. time [s]	solver steps	triggered events
FMU	CADC (Road)	588.91e8	460185.79	-453614.80	10.29	110294	110247
NeuralFMU	CADC (Road)	9.30e8	63558.61	-55610.81	55.09	110301	110247
FMU	WLTC (class 2)	89.82e8	249693.13	-248286.71	13.16	144569	144519
NeuralFMU	WLTC (class 2)	5.67e8	79822.16	15463.58	69.54	144590	144519

consumption on entire cycles, especially the final value of the solution is important and a key factor of model evaluation. Please note, that this final error of the NeuralFMU is more than eight times smaller on training data and even 16 times smaller on validation data. Besides the final error, the NeuralFMU features a much lower MSE (factor ≈ 63 on training, factor ≈ 16 on testing) and maximum error (factor ≈ 7 on training, factor ≈ 3 on testing), but the simulation time increases about five to six times. This is mainly because of the more expensive event-handling inside the hybrid structure and further unused performance optimizations in the prototypical implementation. It can be seen, that the number of events remains unchanged. The number of adaptive solver steps only slightly increases, which indicates that the average system stiffness¹¹ hardly changes. Finally, the training is not converged yet and further training epochs or training on more data (e.g. multiple cycles) may reduce the remaining deviations.

¹¹In this article, an ODE is considered *stiff* if the adaptive step size of the solver is controlled authoritative by the stability objective, instead of the tolerance objective.

4 Conclusion

We highlighted a workflow to allow for hybrid modeling with an industry typical FPM in form of a NeuralFMU. Before training such models, a proper initialization is required. Because initialization of NeuralFMUs is not trivial, we suggested three methods with different requirements: NIPT, CCPT and a topology using ANN/FMU gates, that makes an initialization routine obsolete. The use of this topology was tested in practice using an industry typical FPM, the VLDM. This model features multiple challenges like closed-loops and high-frequent discontinuities. The VLDM was exported in a format that is common in industrial practice, the FMI. On the foundation of the exported FMU, a hybrid model was built up and trained on real measurement data from a chassis dynamometer, including typical measurement errors. The model was trained on only a single driving cycle measurement to show that the presented method is capable of making good predictions on very little data. The trained hybrid model was able to make better predictions compared to the FPM, on training as well as on testing data. To conclude, the presented workflow and software allows for the re-use of already existing industrial models as cores of hybrid models in the form of NeuralFMUs. NeuralFMUs allow for the data-driven modeling of physical effects, that are difficult to model based on first principle, by using the presented methods and techniques.

The briefly highlighted open source library *FMI.jl* allows the easy and seamless integration of FMUs into the Julia programming language. FMUs can be loaded, parameterized, simulated and exported using the abilities of the FMI standard. Optional functions like retrieving the partial derivatives or manipulating the FMU state are available if supported by the FMU. The current library release version is compatible with FMI 2.0 (the common version at the time of release) and initial support for FMI 3.0 is implemented. The library currently supports ME- as well as CS-FMUs, running on Windows and Linux operating systems. Event-handling to simulate discontinuous ME-FMUs is supported. The library extension *FMIFlux.jl* makes FMUs differentiable and opens the possibility to setup and train NeuralFMUs. The framework supports proper event-handling during back-propagation whilst training of discontinuous NeuralFMUs. Beside NeuralFMUs, *FMIFlux.jl* paves the way for other hybrid modeling techniques and new industrial use cases by making FMUs differentiable in an AD-framework. The library repositories are constantly extended by new features and maintained for the upcoming technology progress. Contributors are welcome.

Funding

This research was partially funded by the ITEA3-Project UPSIM (Unleash Potentials in Simulation) N°19006, see: <https://www.upsim-project.eu/> for more information.

Data availability

The used software *FMI.jl* and *FMIFlux.jl* is available open-source under <https://github.com/ThummeTo/FMI.jl> and <https://github.com/ThummeTo/FMIFlux.jl>. The data used in the presented experiment (vehicle measurements) as well as the original model are available for download under https://github.com/TUMFTM/Component_Library_for_Full_Vehicle_Simulations. Further, a tutorial for reconstruction of the presented method focusing on adapting custom use cases will be released soon after this article's publication in the repository of *FMIFlux.jl*.

Acknowledgments

The authors like to thank everyone that contributed to the library repositories, especially our students and student assistants *Josef Kircher*, *Jonas Wilfert* and *Adrian Brune*.

Abbreviations

AD Automatic Differentiation

ANN Artificial Neural Network

BNSDE Bayesian Neural Stochastic Differential Equation

CADC Common Artemis Driving Cycles

CCPT Collocation Pre-Training

CS Co-Simulation

DARN Deep Auto-Regressive Network

FMI Functional Mock-up Interface

FMU Functional Mock-up Unit

FPM First Principle Model

HiL Hardware in the Loop

ME Model Exchange

ML Machine Learning

MSE Mean Squared Error

NEDC New European Driving Cycle

NIPT Neutral Initialization Pre-Training

ODE Ordinary Differential Equation

PAC Probably Approximately Correct

PINN Physics-informed Neural Network

RNN Recurrent Neural Network

SE Scheduled Execution

SSP System Structure and Parameterization

VLDM Vehicle Longitudinal Dynamics Model

WLTC Worldwide harmonized Light-duty vehicles Test Cycle

References

- [1] Jeff Bezanson et al. “Julia: A Fast Dynamic Language for Technical Computing”. In: *CoRR* abs/1209.5145 (2012). arXiv: 1209.5145. URL: <http://arxiv.org/abs/1209.5145>.
- [2] Jeff Bezanson et al. “Julia: A Fresh Approach to Numerical Computing”. In: *CoRR* abs/1411.1607 (2015). arXiv: 1411.1607. URL: <http://arxiv.org/abs/1411.1607>.
- [3] Frederic Bruder and Lars Mikelsons. “Modia and Julia for Grey Box Modeling”. In: Sept. 2021, pp. 87–95. DOI: 10.3384/ecp2118187.
- [4] Tian Qi Chen et al. “Neural Ordinary Differential Equations”. In: *CoRR* abs/1806.07366 (2018). arXiv: 1806.07366. URL: <http://arxiv.org/abs/1806.07366>.
- [5] Benedikt Danquah et al. “Modular, Open Source Simulation Approach: Application to Design and Analyze Electric Vehicles”. In: *2019 Fourteenth International Conference on Ecological Vehicles and Renewable Energies (EVER)*. IEEE, 8.05.2019 - 10.05.2019, pp. 1–8. ISBN: 978-1-7281-3703-2. DOI: 10.1109/EVER.2019.8813568.
- [6] Hilding Elmqvist, Andrea Neumayr, and Martin Otter. “Modia - Dynamic Modeling and Simulation with Julia”. In: *Juliacon 2018*. 2018. URL: <https://elib.dlr.de/124133/>.
- [7] Karol Gregor et al. “Deep AutoRegressive Networks”. In: (2013). DOI: 10.48550/ARXIV.1310.8499. URL: <https://arxiv.org/abs/1310.8499>.
- [8] Lino Guzzella and Antonio Sciarretta. *Vehicle Propulsion Systems: Introduction to Modeling and Optimization*. 3. 3rd ed. 2013. Berlin, Heidelberg: Springer Berlin Heidelberg, 2013. ISBN: 978-3-642-35913-2. URL: <http://nbn-resolving.org/urn:nbn:de:bsz:31-epflucht-1554525>.

- [9] Manuel Haussmann et al. “Learning Partially Known Stochastic Dynamics with Empirical PAC Bayes”. In: (2021). arXiv: 2006.09914 [cs.LG].
- [10] Michael Innes. “Don’t Unroll Adjoint: Differentiating SSA-Form Programs”. In: *CoRR* abs/1810.07951 (2018). arXiv: 1810.07951. URL: <http://arxiv.org/abs/1810.07951>.
- [11] Mike Innes et al. “A Differentiable Programming System to Bridge Machine Learning and Scientific Computing”. In: *CoRR* abs/1907.07587 (2019). arXiv: 1907.07587. URL: <http://arxiv.org/abs/1907.07587>.
- [12] R. E. Kalman. “A New Approach to Linear Filtering and Prediction Problems”. In: *Journal of Basic Engineering* 82.1 (Mar. 1960), pp. 35–45. ISSN: 0021-9223. DOI: 10.1115/1.3662552. eprint: https://asmedigitalcollection.asme.org/fluidsengineering/article-pdf/82/1/35/5518977/35_1.pdf. URL: <https://doi.org/10.1115/1.3662552>.
- [13] Diederik P. Kingma and Jimmy Ba. *Adam: A Method for Stochastic Optimization*. 2014. DOI: 10.48550/ARXIV.1412.6980. URL: <https://arxiv.org/abs/1412.6980>.
- [14] Modelica Association. *Functional Mock-up Interface for Model Exchange and Co-Simulation. Document version: 2.0.2*. Tech. rep. Linköping: Modelica Association, Dec. 2020. URL: <https://github.com/modelica/fmi-standard/releases/download/v2.0.2/FMI-Specification-2.0.2.pdf>.
- [15] Modelica Association. *Functional Mock-up Interface Specification. Document version: 3.0, 2022-05-10*. Tech. rep. Linköping: Modelica Association, May 2022. URL: <https://fmi-standard.org/docs/3.0/>.
- [16] Modelica Association. *System Structure and Parameterization. Document version: 1.0*. Tech. rep. Linköping: Modelica Association, Mar. 2019. URL: <https://ssp-standard.org/publications/SSP10/SystemStructureAndParameterization10.pdf>.
- [17] Christopher Rackauckas et al. “DiffEqFlux.jl - A Julia Library for Neural Differential Equations”. In: *CoRR* abs/1902.02376 (2019). arXiv: 1902.02376. URL: <http://arxiv.org/abs/1902.02376>.
- [18] Rahul Rai and Chandan K. Sahu. “Driven by Data or Derived Through Physics? A Review of Hybrid Physics Guided Machine Learning Techniques With Cyber-Physical System (CPS) Focus”. In: *IEEE Access* 8 (2020), pp. 71050–71073. DOI: 10.1109/ACCESS.2020.2987324.
- [19] M. Raissi, P. Perdikaris, and G.E. Karniadakis. “Physics-informed neural networks: A deep learning framework for solving forward and inverse problems involving nonlinear partial differential equations”. In: *Journal of Computational Physics* 378 (2019), pp. 686–707. ISSN: 0021-9991. DOI: <https://doi.org/10.1016/j.jcp.2018.10.045>. URL: <https://www.sciencedirect.com/science/article/pii/S0021999118307125>.
- [20] J. Revels, M. Lubin, and T. Papamarkou. “Forward-Mode Automatic Differentiation in Julia”. In: *arXiv:1607.07892 [cs.MS]* (2016). URL: <https://arxiv.org/abs/1607.07892>.
- [21] Elisabeth Roesch, Chris Rackauckas, and Michael Stumpf. “Collocation based training of neural ordinary differential equations”. In: *Statistical Applications in Genetics and Molecular Biology* 20 (July 2021). DOI: 10.1515/sagmb-2020-0025.
- [22] Tobias Thummerer, Lars Mikelsons, and Josef Kircher. “NeuralFMU: towards structural integration of FMUs into neural networks”. In: *Proceedings of 14th Modelica Conference 2021, Linköping, Sweden, September 20-24, 2021*. Ed. by Martin Sjölund et al. 2021. ISBN: 978-91-7929-027-6. DOI: 10.3384/ecp21181297.
- [23] Tobias Thummerer, Johannes Tintenherr, and Lars Mikelsons. “Hybrid modeling of the human cardiovascular system using NeuralFMUs”. In: *Journal of Physics: Conference Series* 2090.1 (2021), p. 012155. DOI: 10.1088/1742-6596/2090/1/012155.
- [24] Evren Mert Turan and Johannes Jäschke. “Multiple Shooting for Training Neural Differential Equations on Time Series”. In: *IEEE Control Systems Letters* 6 (2022), pp. 1897–1902. DOI: 10.1109/LCSYS.2021.3135835.
- [25] Jared Willard et al. “Integrating Physics-Based Modeling with Machine Learning: A Survey”. In: (2020). arXiv: 2003.04919 [physics.comp-ph].